Supporting Information for

Graphene Oxide Precursor effects on 3D-Printed Carbon Scaffold

Megan C. Freyman,[‡a] Xinzhe Xue,[‡ b] Dun Lin,[b] Yat Li,[b] Marcus Worsley[a] and Swetha Chandrasekaran[a *]

a. Material Science Department, Lawrence Livermore National Lab, Livermore, California, 94551, United States. Email: chandrasekar2@llnl.gov

b. Department of Chemistry and Biochemistry, University of California, Santa Cruz California, 95064, United States

‡ These authors contributed equally to this work.

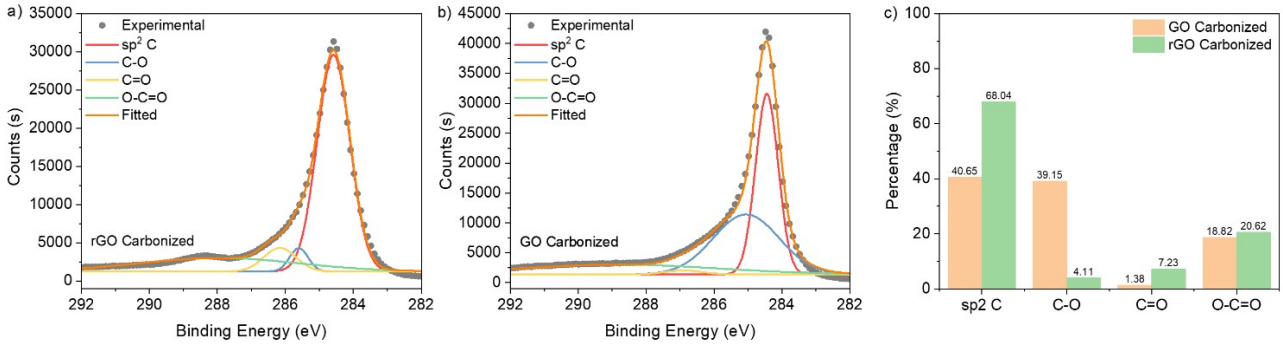

Figure S1. C1s XPS spectrum of carbonized GO (a) and rGO (b) carbon scaffolds Percentage of different functional groups (c) carbonization.

Hydroxypropyl methyl cellulose (HPMC) has been successfully used with GO suspensions to produce a printable ink.[1] However, when HPMC was mixed with rGO suspensions, it is difficult to produce a printable ink. To address this issue, nanocrystalline cellulose (CNC) was used instead. When HPMC is substituted for CNC in the rGO ink, the ink becomes too stiff to print, leading to clogging issues, as demonstrated by the increased storage modulus by 80% (**Figure S2a**). SEM images of rGO with 18 wt% HPMC (**Figure S4**) reveal a significant change in pore structure compared to rGO with 18 wt% CNC, as shown in **Figure 1a-c**. The pore structure appears denser and less loose when HPMC is used in the rGO ink. The aerogel made with rGO and 18wt% HPMC achieved BET surface area of 222 m^2g^{-1}. This indicates that the interaction between cellulose and the rGO precursor significantly affects the resulting material properties **Figure S4**. Based on the hysteresis nitrogen adsorption and desorption isotherms in **Figure S4** some mesoporosity is preserved but there is a shift in the pore width distribution (**Figure S4b**) to smaller pores compared to the standard rGO 18wt% CNC aerogel (**Figure 3b**). Based on this structural difference between the rGO aerogel made with CNC compared with an aerogel made with HPMC shows how the cellulose viscosifier can influence the final structure of the carbonized aerogel.

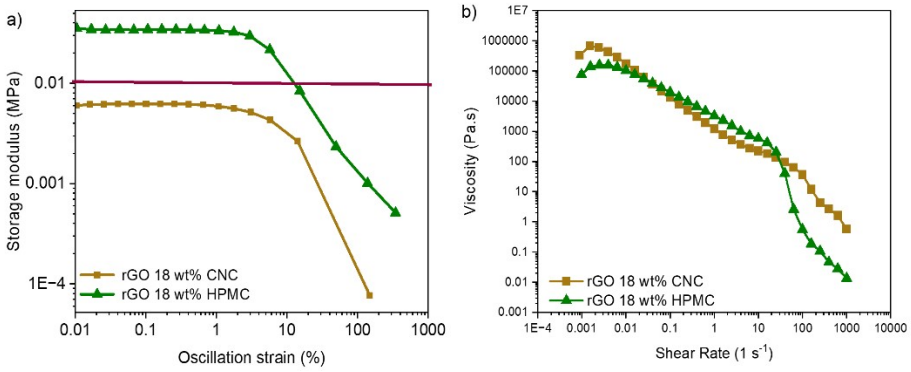

Figure S2 Comparison between rGO 18wt% CNC standard ink and modified rGO 18wt% HPMC. (a) storage modulus Red line indicates maximum range for printable storage modulus for our printing conditions and (b) viscosity.

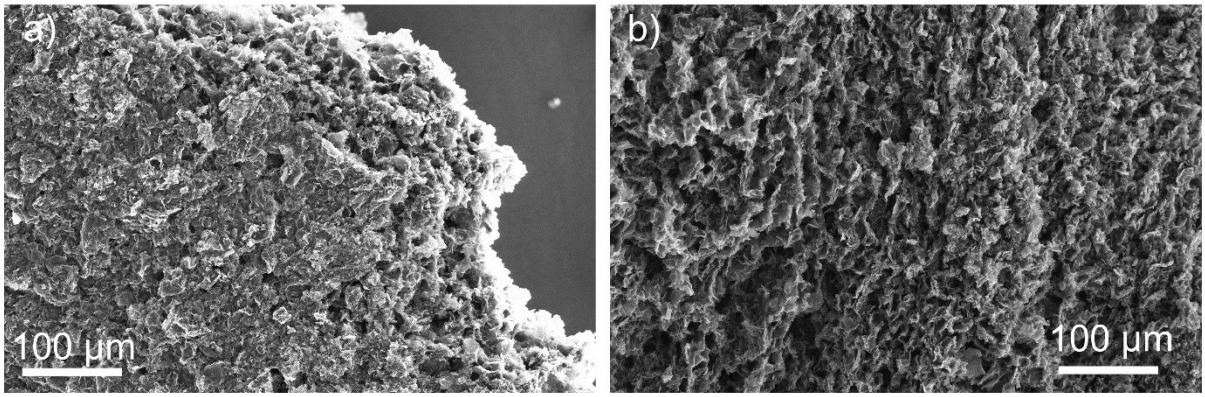

Figure S3 SEM rGO 18wt% CNC pucks (a) surface and (b) cross section.

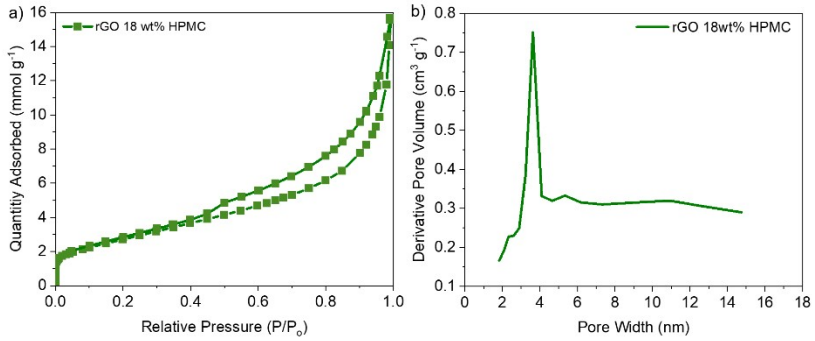

Figure S4 (a) Nitrogen adsorption and desorption isotherm and (b) pore size distribution for rGO 18 wt% HPMC

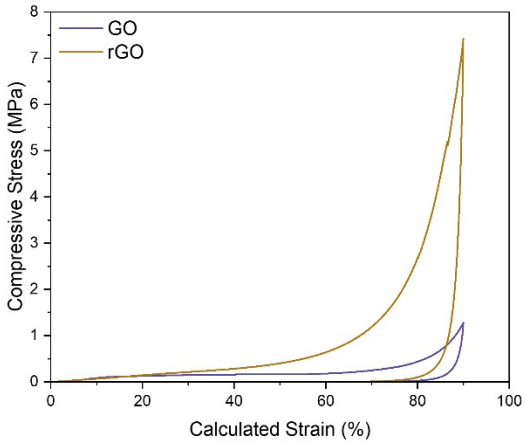

Figure S5. 90% Compression of GO and rGO aerogels.

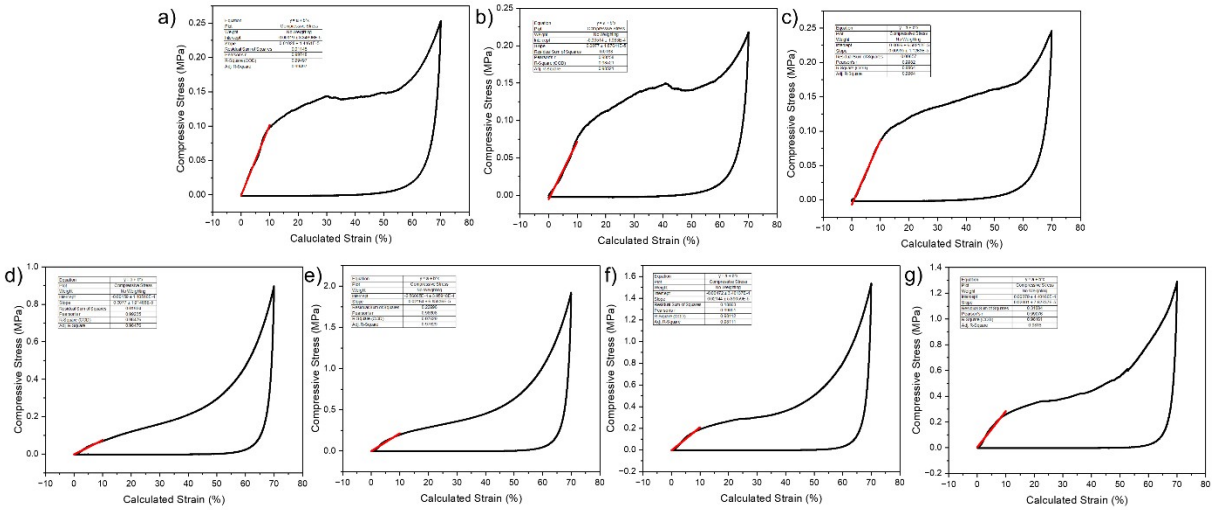

Figure S6. 70% compression stress strain plots of (a)-(c) GO and (d) – (f) of rGO.

The specific modulus was calculated: first by finding the geometric density for each sample. Then the compressive modulus was found from the first 10% region of each 70% compressive stress strain curve. The compressive modulus was then divided by the geometric density to give the specific modulus.

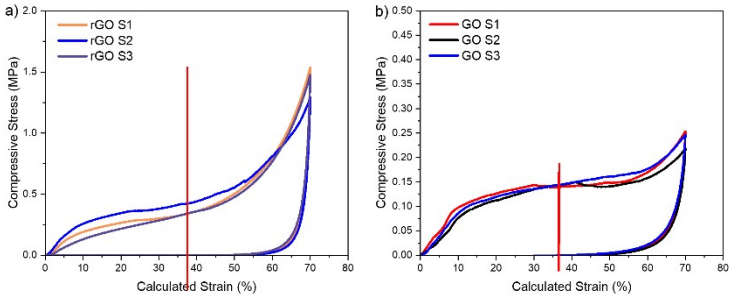

Figure S7. 70% Compression of (a) rGO and (b) GO standard ink samples where the red line shows where the compressive stress value was taken to be used in **Equation 1**.

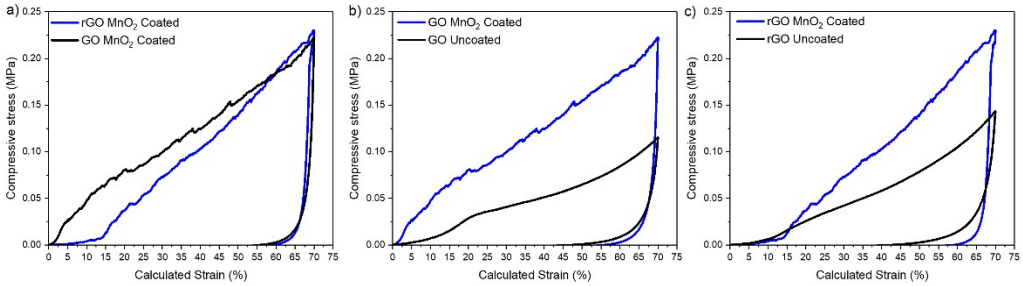

Figure S8. Comparison of MnO2-coated and uncoated 3D-printed aerogels under 70% compression. (a) Comparison between rGO-coated and GO-coated aerogels, (b) Comparison of GO-coated and uncoated aerogels, (c) Comparison of rGO-coated and uncoated aerogels.

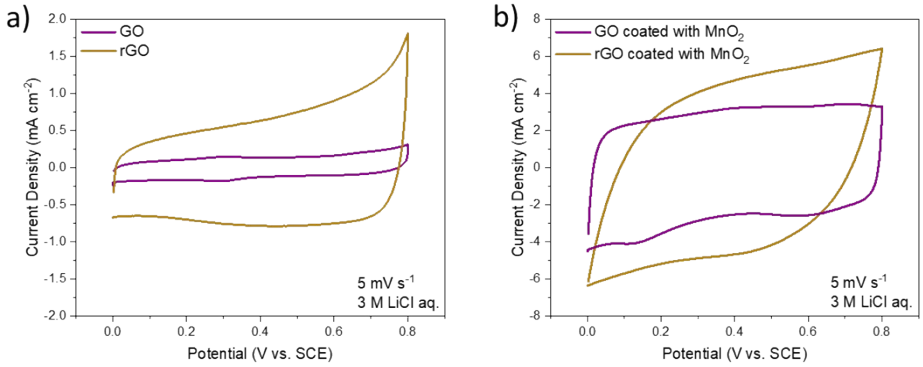

Figure S9. Cyclic Voltammetry curves of (a) bare 3D printed GO and rGO carbon scaffold aerogel and (b) carbon scaffolds coated with MnO_2.

As Figure S10 shows, the 1 V symmetric device fabricated using printed rGO aerogels coated with MnO_2 not only delivers higher capacitance of 722 mF cm^{-2}, but also higher rate retention rate of 77.97 %. This indicates that the rGO substrates promotes MnO_2 pseudocapacitive charge storage.

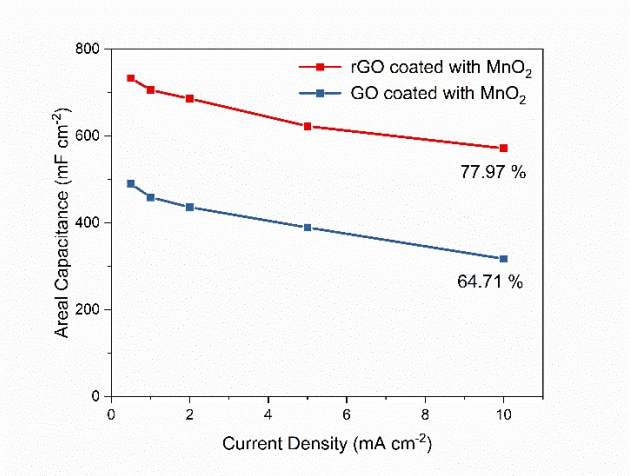

Figure S10. Rate performance of two-electrode symmetric device fabricated using both GO and rGO coated with MnO_2.

As shown in the figure, the symmetric device stably operates for 20000 cycles under 100 mV s^{-1}, and maintains the high retention rate of 97.27 %.

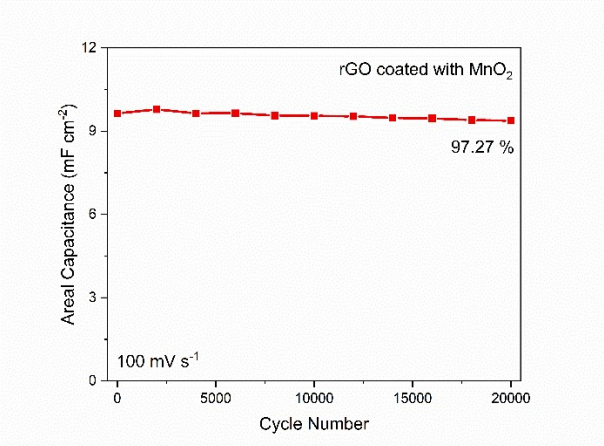

Figure S11. Long term stability of the symmetric device using rGO coated with MnO_2.

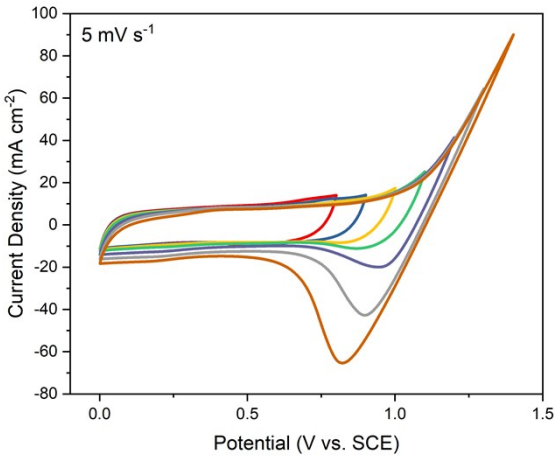

Figure S12 Cyclic voltammetry measurements of 3DrGO electrode coated with MnO_2 under different potential windows.

As shown in **Figure S13a**, the MnO_2/rGO symmetric device maintains 83.26 % capacity retention after 2,000 cycles, demonstrating robust stability even at low rates. Furthermore, we also performed a floating test at 0.5 mA cm^{-2} (**Figures S13b** and **S13c**). Following a 2-hour floating period at 1 V, the device maintains comparable GCD profiles and discharge times, confirming the high voltage tolerance of the rGO substrates in this configuration.

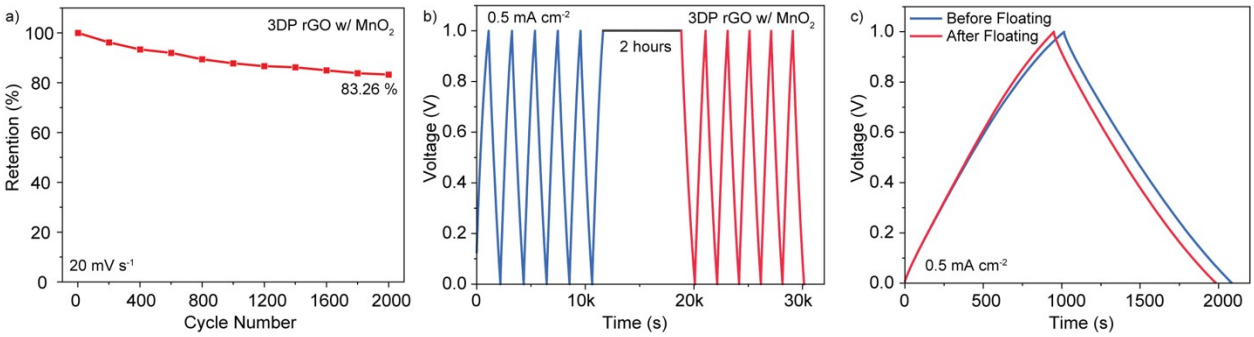

Figure S13 (a) stability test, (b) floating cycling, and (c) GCD curves before and after floating tests of the symmetric MnO_2/rGO device.

References

1 B. Yao, S. Chandrasekaran, H. Zhang, A. Ma, J. Kang, L. Zhang, X. Lu, F. Qian, C. Zhu, E. B. Duoss, C. M. Spadaccini, M. A. Worsley and Y. Li, *Advanced Materials*, 2020, **32**, 1906652.